Radar Performance of the OFDM Directional Modulation Waveforms for Joint Radar-Communication

Citation for published version:
Zhang, K, Huang, G, Ouyang, S, Ding, Y & Li, X 2024, Radar Performance of the OFDM Directional Modulation Waveforms for Joint Radar-Communication. in *2023 Cross Strait Radio Science and Wireless Technology Conference (CSRSWTC).*, 10427127, IEEE, 2023 Cross Strait Radio Science and Wireless Technology Conference, Guilin, China, 10/11/23. https://doi.org/10.1109/csrswtc60855.2023.10427127

Digital Object Identifier (DOI):
10.1109/csrswtc60855.2023.10427127

Document Version:
Peer reviewed version

Published In:
2023 Cross Strait Radio Science and Wireless Technology Conference (CSRSWTC)

Radar Performance of the OFDM Directional Modulation Waveforms for Joint Radar-Communication

Kailuo Zhang 1), Gaojian Huang*1), Shan Ouyang 2), Yuan Ding 3), Xingwang, Li 1)
1) School of Physics and Electronic Information Engineering, Henan Polytechnic University, Jiaozuo 454003, China
2) School of Information and Communications, Guilin University of Electronic Technology, Guilin 541004, China
3) Institute of Sensors, Signals and Systems (ISSS), Heriot-Watt University, Edinburgh EH14 4AS, U.K
*Corresponding author: g.huang@hpu.edu.cn

***Abstract*—The orthogonal frequency-division multiplexing (OFDM) waveforms have been intensively studied for joint Radar-communication (JRC), which can provide high data rates for wireless communication, and the range-doppler information of the Radar target also can be estimated. In this paper, the OFDM directional modulation (OFDM-DM) waveforms are proposed for the JRC, and its radar performance is investigated by a correlation-based Radar signal processing approach. It has been shown that compared with the OFDM JRC scheme the proposed OFDM-DM waveforms can suppress the interference from the non-target directions, which is validated via the simulation results.**

Keywords—Correlation-based Radar signal processing; interference suppression; joint Radar-communication (JRC); orthogonal frequency-division multiplexing directional modulation (OFDM-DM)

I. INTRODUCTION

Joint Radar-Communication (JRC) is a promising technique in 5G-and-Beyond (B5G) application scenarios such as autonomous vehicles and military Radar systems [1], [2]. The JRC systems can achieve Radar and wireless communication functions simultaneously by sharing the spectrum resources in a single hardware platform. Thus, the mutual interference between Radar sensing and communication can be eliminated and the pressure on scarce spectrum resource available will be alleviated. Moreover, these two functions can also assist each other. For example, the Radar sensing of the environment surroundings could be used for more accurate beamforming towards the legitimate users [3]. The main challenge in the JRC research is the waveform design, which must simultaneously deliver information and achieve Radar sensing. The orthogonal frequency-division multiplexing (OFDM) signal is viewed as the most popular JRC waveform that has been intensively studied due to its high data rates in V2V application scenarios [4]. However, the OFDM JRC waveforms suffer the problem of interference from the non-target directions. In order to cancel the interference, high-complexity algorithms need to be adopted, which would require extremely high computational efforts [5].

In this paper, we first propose OFDM directional modulation (OFDM-DM) JRC waveforms, which can automatically suppress the backscattering interference signals from the non-target directions. Here the DM refers to a transmitter technology that can project the digitally encoded information signals into a desired spatial direction while simultaneously distorting the constellation formats of the same signals in all other directions [6–8]. Generally, the DM is used in physical-layer secure wireless communications. When it is employed for JRC, it can not only inherit the superiority of DM but also can achieve better Radar performance compared with the conventional OFDM JRC scheme.

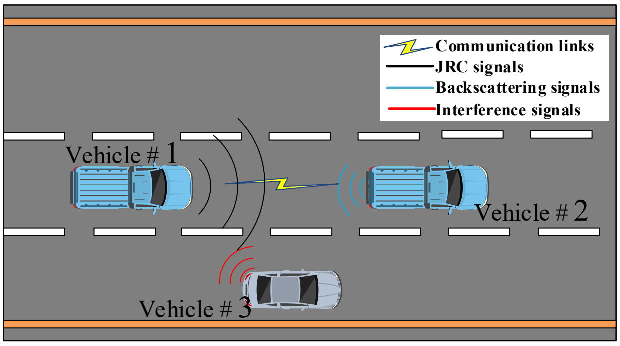

Fig. 1. An example of the V2V JRC application scenario.

II. PROPOSED OFDM-DM JRC

A. JRC Application Scenarios

In Fig.1, an example of JRC V2V application scenario is depicted. In the example, vehicles #1 and #2 are equipped with JRC devices and each JRC device includes a transmitter and a receiver. The vehicle #1 transmits an information signal, i.e., $S(t)$, to target vehicle #2, meanwhile vehicle #1 needs to estimate the range to the target vehicle #2. Here vehicle #3 is viewed as a car which backscatters interference signals.

B. OFDM-DM JRC Transmitters

In Fig. 2, the transmitter architecture consisting of an N-element OFDM-DM JRC antenna array is depicted. The input OFDM signal is first divided into N copies and each copy is connected to a single-pole three-throw switch radio frequency (RF) switch (with '+1', '0' and '–1' respectively representing 'ON', 'OFF' and 'Flipping') after a phase delay then radiated

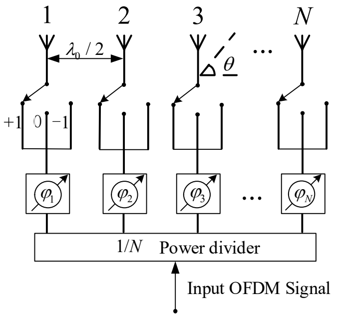

Fig. 2. The architecture of the proposed OFDM-DM transmitter.

into free space. It is assumed that each active antenna element is identical and has isotropic radiation pattern. Here the elements are uniformly spaced with $\lambda_0/2$, where λ_0 is the wavelength corresponding to the lowest OFDM sub-carrier f_0. The transmitted signals in free space can be expressed as

$$S(\theta,t)=\frac{1}{\sqrt{N}}\sum_{n=1}^{N}\left(x(t)\cdot e^{j\varphi_n}\cdot W_n(t)\cdot e^{j(n-1)\pi\cos\theta}\right), \tag{1}$$

where $W_n(t)$ represents the nth RF switch function in the time domain, see Fig. 3. φ_n denotes the phase delay in the nth antenna branch and in order to achieve beamforming gain towards the target direction θ_0, φ_n is configured as $-(n-1)\pi\cos\theta_0$. For better illustration, considering $x(t)$ denotes an OFDM symbol, which can be expressed as

$$x(t)=\frac{1}{\sqrt{K}}\sum_{k=1}^{K}D_k\cdot e^{j2\pi\left[f_0+(k-1)f_p\right]t}, \tag{2}$$

where D_k denotes the complex modulated symbol applied upon the kth sub-carrier. K denotes the total number of OFDM subcarriers. $1/\sqrt{K}$ is used for the power normalization. f_p denotes the sub-carrier frequency spacing. $W_n(t)$ can be expanded using the Fourier series. Thus, $S(\theta, t)$ can be rewrite as

$$S(\theta,t)=\frac{x(t)}{\sqrt{NK}}\cdot\sum_{q=-\infty}^{\infty}\left[\underbrace{e^{j2q\pi f_p t}\sum_{n=1}^{N}\left(\left(\frac{\sin\left(q\pi\Delta\sigma_n^{(1)}\right)}{q\pi}-\frac{\sin\left(q\pi\Delta\sigma_n^{(2)}\right)}{q\pi}\right.\right.}_{\chi\left(q,N,\sigma_n^s,\Delta\sigma_n^{(1)},\Delta\sigma_n^{(2)},t,\theta\right)}, \tag{3}$$

$$\left.\underbrace{\left.\left.\cdot e^{-jm\pi\left(\Delta\sigma_n^{(1)}+\Delta\sigma_n^{(2)}\right)}\right)\cdot e^{-jq\pi\left(2\sigma_n^s+\Delta\sigma_n^{(1)}\right)}\right)\cdot e^{j(n-1)\pi(\cos\theta-\cos\theta_0)}}\right]$$

where q represents the Fourier coefficient and $\sigma_n^s=t_n^s/T_p$, $\Delta\sigma_n^{(1)}=\Delta t_n^{(1)}/T_p$, and $\Delta\sigma_n^{(2)}=\Delta t_n^{(2)}/T_p$. In this scheme, σ_n^s, $\Delta\sigma_n^{(1)}$ and $\Delta\sigma_n^{(2)}$ are configured as

$$\begin{cases}\Delta\sigma_n^{(1)}\neq\Delta\sigma_n^{(2)}\\ \Delta\sigma_n^{(1)},\Delta\sigma_n^{(2)},\sigma_n^s\in\left\{\dfrac{w-1}{N}\middle|w=1,2,\ldots,N\right\}\\ \sigma_i^s\neq\sigma_j^s,\Delta\sigma_i^{(1)}=\Delta\sigma_j^{(1)},\Delta\sigma_i^{(2)}=\Delta\sigma_j^{(2)},\ when\ i\neq j\end{cases}. \tag{4}$$

Thus, along the target's direction θ_0, the radiated signals can be expressed as $(\Delta\sigma^{(1)}-\Delta\sigma^{(2)})\cdot\sqrt{N}\cdot x(t)$ with $\Delta\sigma_n^{(1)}=\Delta\sigma^{(1)}$ and $\Delta\sigma_n^{(2)}=\Delta\sigma^{(2)}$. While when $\theta\neq\theta_0$, the OFDM symbols in free space will be distorted by the function of $\chi(\cdot)$. For example, the transmitted signal waveforms at the hth (h = 1, 2, …, K) subcarrier can be expressed as

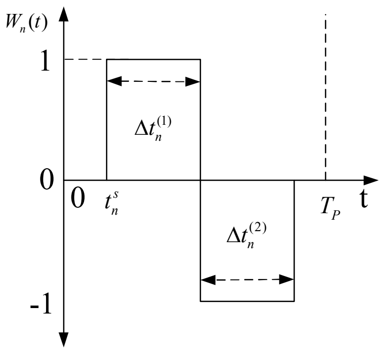

Fig. 3. An example RF switch function $W_n(t)$ in time domain.

$$S_h(\theta\neq\theta_0,t)=\frac{1}{\sqrt{NK}}\cdot\sum_{k=1}^{K}\left[D_k\cdot e^{j2\pi\left[f_0+(k-1)f_p\right]t}\right.$$
$$\left.\cdot\chi\left(q=h-k,N,\sigma_n^s,\Delta\sigma_n^{(1)},\Delta\sigma_n^{(2)},t,\theta\right)\right]. \tag{5}$$

Note that in the JRC application scenario, the transmitter and the receiver are co-located. At the receiver, it is assumed that it only has a single antenna element used to receive the signals scattered back.

C. Correlation-Based Radar Range Images

In Fig.1, when the JRC signal radiates from the vehicle #1, the radiated signal would be scattered back from the vehicles #2 and #3. Here the range to the target vehicle #1 and the interference car #3 are assumed to be R_{tar} and R_{inter}, respectively. Thus, the received signal $y(t)$ at the vehicle #1 can be expressed as

$$y(\theta_0,\theta_{\text{inter}},t)=\gamma_1 S\left(\theta_0,t-\frac{2R_{\text{tar}}}{c_0}\right)+\gamma_2 S\left(\theta_{\text{inter}},t-\frac{2R_{\text{inter}}}{c_0}\right), \tag{6}$$

where γ_1 and γ_2 denote attenuation coefficients, and c_0 is the speed of the light. θ_{inter} denotes the direction of the interference source. When a correlation processing approach is adopted for Radar range measurement, the cross-correlation function $r_{yx}(\theta_0, \theta_{\text{inter}}, \tau)$ can be expressed as

$$r_{yx}(\theta_0,\theta_{\text{inter}},\tau)=\int_0^{\infty}y(\theta_0,\theta_{\text{inter}},t)x^*(t-\tau)dt, \tag{7}$$

Substituting (2), (3), (4), and (6) into (7), we get

$$r_{yx}(\theta_0,\theta_{\text{inter}},\tau)=\gamma_1\cdot\left(\Delta\sigma^{(1)}-\Delta\sigma^{(2)}\right)\cdot\sqrt{N}\cdot\int_0^{\infty}x\left(t-\frac{2R_{\text{tar}}}{c_0}\right)x^*(t-\tau)dt$$
$$+\frac{\gamma_2}{\sqrt{N}}\int_0^{\infty}\left(x\left(t-\frac{2R_{\text{inter}}}{c_0}\right)\cdot x^*(t-\tau)\right.$$
$$\left.\cdot\sum_{q=-\infty}^{\infty}\chi\left(q,N,\sigma_n^s,\Delta\sigma_n^{(1)},\Delta\sigma_n^{(2)},t-\frac{2R_{\text{inter}}}{c_0},\theta_{\text{inter}}\right)\right)dt. \tag{8}$$

From (8), obviously, the interference signals from the non-target directions would be suppressed since $S(\theta_{\text{inter}}, t)$ is a random function, thus, a low or even zero correlation between functions of $S(\theta_{\text{inter}}, t)$ and $x(t)$. Noted here for simplicity, only a single OFDM symbol is considered for the correlation-based processing analysis.

III. Simulation Results and Discussions

In order to validate the effectiveness of the proposed OFDM-DM JRC scheme, the Radar range of the vehicle target is estimated by using the correlation-based processing approach. In the simulation example, it is assumed that $R_{\mathrm{tar}} = 45$ m, $R_{\mathrm{inter}} = 30$ m, $\theta_0 = 90°$, $\theta_{\mathrm{inter}} = 30°$. Meanwhile, we set $N = 16$, $f_p = 312.5$ kHz, $K = 64$ and each sub-carrier is quadrature phase shift keying (QPSK) modulated. The channel is assumed to be additive white Gaussian noise and the signal-to-noise ratio (SNR) is set to be 20 dB.

In Fig. 4. the Radar range profiles are depicted. It can be observed that peaks occur at the range of 30 m in both OFDM and OFDM-DM JRC waveform schemes, suggesting that the information of range can be obtained by both waveform schemes. However, in the conventional OFDM JRC scheme, at the range of 30 m, a high side-lobe at a level of around –5 dB occurs, indicating another Radar target could exist, which would result in target ambiguity. This is because of the interference signal being scattered back from the car, i.e., the vehicle # 3, seen in Fig. 1. While, in the OFDM-DM JRC scheme, it can be observed that the range to the target vehicle, i.e., R_{tar}, can be estimated without the issue of target ambiguity. The first sidelobe at the level of around –15 dB, and at the range of 30 m, a null occurs, indicating the interference signals being scattered from the vehicle # 3 are completely suppressed.

In Fig. 5, the bit error rate (BER) spatial distributions of the proposed OFDM-DM JRC scheme are simulated and compared with that in the conventional OFDM JRC scheme at SNR = 20 dB. Here the SNR is measured along θ_0, and the noise power is assumed to be identical along every direction. It can be observed that in the proposed OFDM-DM JRC scheme, the BER main beam can be shaped only along the direction of the target vehicle, suggesting the information can be intercepted along 90°, while along other directions, the low BER sidelobe levels indicate information cannot be eavesdropped. In contrast, in the OFDM JRC scheme, the high BER sidelobe levels distributed in the spatial domain indicate information can be easily eavesdropped along these directions. Thus, the proposed OFDM-DM JRC scheme can not only suppress interference but also secure the information to the target.

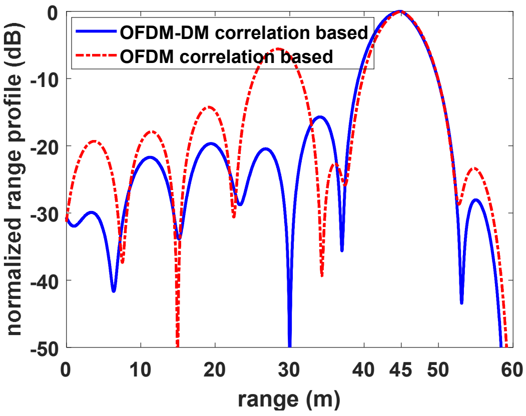

Fig. 4. Radar range profiles of the OFDM and the proposed OFDM-DM JRC schemes with the correlation-based processing approach at SNR level of 20 dB. R_{tar} and R_{inter} are respectively set to be 45 m and 30 m.

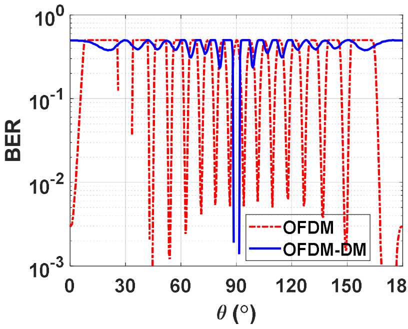

Fig. 5. Simulated BER spatial distributions of QPSK modulated OFDM and the proposed OFDM-DM JRC schemes with SNR = 20 dB.

IV. Conclusions

In this paper, a novel JRC waveform, namely, OFDM-DM, was proposed. It has been shown that the proposed OFDM-DM waveform scheme can suppress interference from the non-target directions without consuming additional computational resources. That is of great significance in JRC application scenarios with high interference environments. In addition, the proposed OFDM-DM JRC also inherits the advantages of DM, which can secure information transmissions along the target directions.

Acknowledgment

Dr. G. Huang’s work was supported by the Fundamental Research Funds for the Universities of Henan Province under Grant NSFRF230421. Dr Yuan Ding’s work was supported by EPSRC (UK) under the Grant EP/V002635/1.

References

[1] J. A. Zhang, M. L. Rahman, K. Wu, X. Huang, Y. J. Guo, S. Chen, and J. Yuan, “Enabling joint communication and radar sensing in mobile networks—A survey,” *IEEE Commun. Surveys Tuts.*, vol. 24, no. 1, pp. 306–345, 1st Quart. 2022.

[2] Y. Cui, F. Liu, X. Jing, and J. Mu, “Integrating sensing and communications for ubiquitous IoT: Applications, trends, and challenges,” *IEEE Netw.*, vol. 35, no. 5, pp. 158–167, Sep./Oct. 2021.

[3] D. K. Pin Tan, J. He, Y. Li, A. Bayesteh, Y. Chen, P. Zhu, and W. Tong, “Integrated sensing and communication in 6G: Motivations, use cases, requirements, challenges and future directions,” in Proc. 1st IEEE Int. *Online Symp. Joint Commun. Sens. (JC&S)*, 2021, pp. 1–6.

[4] C. Sturm and W. Wiesbeck, “Waveform design and signal processing aspects for fusion of wireless communications and radar sensing,” *Proc. IEEE Proc. IRE.*, vol. 99, no. 7, pp. 1236–1259, Jul. 2011.

[5] Y. L. Sit, B. Nuss, and T. Zwick, “On mutual interference cancellation in a MIMO OFDM multiuser radar-communication network,” *IEEE Veh. Technol. Mag.*, vol. 67, no. 4, pp. 3339–3348, Apr. 2018.

[6] Y. Ding and V. F. Fusco, “A Vector Approach for the Analysis and Synthesis of Directional Modulation Transmitters,” *IEEE Trans. Antennas Propag.*, vol. 62, no. 1, pp. 361–370, Jan. 2014.

[7] G. Huang, S. Chen, Y. Ding, X. Li, A. Nallanathan and S. Mumtaz, “Security-enhanced directional modulation symbol synthesis using high efficiency Time-Modulated Arrays,” *IEEE Trans. Veh. Technol.*, pp. 1–6, Aug. 2023.

[8] G. Huang, Y. Ding, S. Ouyang, and V. Fusco, “Three-state time-modulated array-enabled directional modulation for secure orthogonal frequency-division multiplexing wireless transmission,” *IET Commun.*, vol. 16, no. 19, pp. 2321–2327, Sep. 2022.